

# BIRL: Benchmark on Image Registration methods with Landmark validation

Jiri Borovec

FEE, Czech Technical University in Prague

jiri.borovec@fel.cvut.cz

**Abstract.** *This report presents a generic image registration benchmark with automatic evaluation using landmark annotations. The BIRL framework has a few key features, such as: easily extendable, performance evaluation, parallel experimenting, simple visualisations, experiment's time-out limit, pause/resume experiments. The main use-cases are (a) compare your (newly developed) method with some State-of-the-Art (SOTA) methods on a common dataset and (b) experiment SOTA methods on your custom dataset (which should contain landmark annotation).*

*In this paper, we present mixed-methods aiming at bio-medical imaging and experimental result on CIMA dataset. However, any other methods for other domain can be added or costume dataset to be used.*

<https://borda.github.io/BIRL>

## 1. Introduction

The image registration is a crucial task in many domains and task, although we will focus here on bio-medical image registration [8, 14, 20, 23, 26].

In Digital Pathology, one of the most simple and yet most useful features is the ability to view serial sections of tissue simultaneously on a computer monitor [5, 15, 17, 18, 25]. This enables the pathologist to evaluate the histology and expression of multiple markers for a patient in a single review [24]. However, the rate-limiting step in this process is the time taken for the pathologist to open each individual image, align the sections within the viewer, and then manually move around the section. In addition, due to tissue processing and pre-analytical steps, sections with different stains have non-linear variations between the two acquisitions. That is, they will stretch and change shape from section to section. [3, 9, 10, 12, 22]

In recent years we notice quite high luck of fair comparison of newly developed methods with well-established methods for the particular domain. It was the primary motivation to collect and annotated a histology dataset of microscopy images and develop an image registration evaluation framework to fill this gap.

## 2. BIRL framework

The BIRL is a light-weighted Python framework for simple image registration experimentation/benchmarking on landmarks-like annotated datasets.

Let us summarise the main/key features of this framework/package:

- automatic execution of image registration of a sequence of image pairs
- integrated evaluation of registration performances using Target Registration Error (TRE)
- integrated visualisations of performed registration
- running several image registration experiment in parallel
- resuming unfinished sequence of registration benchmark
- handling around dataset and creating own experiments
- using basic image pre-processing - normalising
- rerun evaluation and visualisation for finished experiments

### 2.1. Benchmark workflow

Then core benchmark *class* is designed to be inherited and just needed experimental calls are overwritten in particular (*child*) image registration method. In particular, the benchmark workflow is the following:

1. preparing the experiment, e.g. create experiment folder, copy configurations, etc.
2. loading required data - the experiment cover file
3. performing the sequence of experiments (optionally in parallel) and save experimental results (registration outputs and partial statistic) to a common table and optionally do particular visualisation of performed experiments
4. evaluating results of all performed experiments
5. summarising and export results from the complete benchmark.

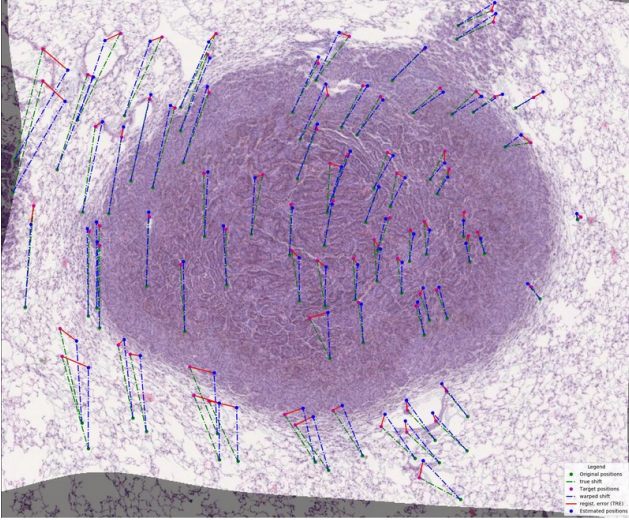


Figure 1. Sample visualisation of TRE.

## 2.2. Metrics

Assume that we have set of landmarks (key points)  $L^F$  and  $L^M$  in target  $I^F$  and source  $I^M$  image respectively and  $\mathbf{x}^F \in L^F$  and  $\mathbf{x}^M \in L^M$  marking the same biological structure in both images. More over we have a set of warped  $\hat{\mathbf{x}}^M$  from  $\mathbf{x}^M$  to match  $\mathbf{x}^F$ .

The evaluation is based on Target Registration Error (TRE) between two sets of landmarks  $\mathbf{x}^F$  and  $\hat{\mathbf{x}}^M$  in the two registered images - target and warped images with its landmarks. Lets us denote

$$TRE = d_e(\mathbf{x}_l^F, \hat{\mathbf{x}}_l^M)$$

where  $\mathbf{x}^F$  and  $\hat{\mathbf{x}}^M$  are the landmark coordinates in the target and warped image and  $d_e(\cdot)$  is the Euclidean distance. As image sizes differs and it makes an wider comparison uneasy, all TRE are normalised by the image diagonal relative TRE,

$$rTRE = \frac{TRE}{diag}$$

where diag image diagonal.

Let us also denote following aggregation measures  $a_d(\cdot) = \text{mean}_{\text{dataset}}(\cdot)$ ,  $m_i(\cdot) = \text{median}_{\text{image}}(\cdot)$ ,  $s_i(\cdot) = \text{max}_{\text{image}}(\cdot)$ . The motivation for using the median is not to penalise a few inaccurate landmarks if most of them are registered well.

We introduce a robustness  $R$  as a relative value how many landmarks  $L$  improved its TRE by performed registration compared to the initial TRE, otherwise, formally

$$R = 1/|L| \sum_j TRE_j^{\text{regist}} < TRE_j^{\text{init}}$$

All missing or incomplete registrations in the submission are considered to have the initial TRE.

## 2.3. Typical use-cases

We have identified the two main use-cases of this framework how the user can get the most of already done work with minimal effort.

**Comparing with SOTA on a common dataset.** The quite common problem of newly developed methods is just presenting their new method on their private dataset, which is not well described also usually very small. This missing comparison with SOTA methods on the common (well described) dataset can be fixed by integrating new methods to the BIRL framework, run the benchmark and compare new results with the presented scores. For this case user need only to overwrite methods/function which is essential to each particular image registration method:

- `_prepare_img_registration(...)` if some extra preparation before running own image registrations are needed. [before each image registration experiment]
- `_execute_img_registration` execute/perform the image registration, time of this methods is measured as execution time. In case you call external method from command line, just rewrite `_generate_regist_command(...)` which prepare the registration command to be executed, also you can add generating complete registration script/macro if needed. [core of each image registration experiment]
- `_extract_warped_image_landmarks(...)` extract the required warped landmarks or perform landmark warping in this stage if it was not already part of the image registration. [after each image registration experiment]
- `_clear_after_registration(...)` removing some temporary files generated during image registration. [after each image registration experiment]

**Exploring SOTA methods on a custom dataset.** This is another practical use-case, especially for bio-medical experts obtaining new data. The user may ask a question about what is the best method for registering these images together. Then he can prepare dataset file - CSV table, where each row contains a path to the source and target image and their landmarks annotation. (if a performance evaluation/analyses are not needed, the landmark annotation can be omitted).

## 3. Experiments

With the framework in our hands, we need to add dome State-Of-The-Art (SOTA) methods and run them on standard/prepared dataset. We start with brief decoration of already integrated SOTA methods, followed by recapitulation on CIMA dataset and finishing with presenting result of SOTA methods on this dataset (also showing visualisations by this framework).<sup>1</sup>

<sup>1</sup>Note that some of the following methods also offer other configuration of selected transformation, metric, optimisation, etc. which is easily accessible in configurations file inside the BIRL framework.

### 3.1. SOTA methods

There are many standards or widely used methods/software/frameworks for biomedical image registration. We stick only with publicly available ones, and also we require that the implementation produce warped landmarks for evaluation.

**Advanced Normalisation Tools (ANTs) [2]** is a registration toolkit using ITK as a backend aiming at MR imaging. The ANTs allows creating custom image registration pipeline composed of several transformations and similarity measures in a multi-scale scheme. *In this experiment, we used a combination of affine registration with Mattes mutual information (MMI) followed by SyN registration with Cross-Correlation (CC) similarity measure.*

**bUnwarpJ [1]** is a ImageJ/Fiji [21] plugin which estimates a symmetric non-linear B-spline-based deformation. The minimised criterion is a sum of squares difference (SSD) in a multiresolution way.

**DROP [6,7]** differs from most other methods by using discreet optimisation (solving efficiently in a multiresolution fashion using linear programming) for minimising a sum of absolute differences (SAD) criterion.

**Elastix [11]** is an image registration software base on the Insight Segmentation and Registration Toolkit (ITK)<sup>2</sup> offering several transformations/metrics/optimisations in multi-resolution scheme. *In this experiment we used b-spline image registration by Adaptive Stochastic Gradient Descent minimising Advanced MMI optimised.*

**NiftyReg [16, 19]** open-source software performs linear or nonlinear registration for two and three dimensional images. The linear registration is based on a block-matching technique, and the non-linear is following the Free-Form Deformation scheme. *In this experiment, we used R wrapper to this software and defined two-step registration - linear and non-linear.*

**Register virtual stack slices (RVSS) [1]** is another ImageJ/Fiji registration plugin which extends the bUnwarpJ and relies on SIFT [13] feature points offering several deformation types.

### 3.2. CIMA dataset

The dataset<sup>3</sup> [4] consists of 2D histological microscopy tissue slices, stained with different stains, and landmarks denoting key-points in each slice. The main challenges for these images are the following: (i) enormous image size,

<sup>2</sup><https://itk.org>

<sup>3</sup><http://cmp.felk.cvut.cz/~borovji3/?page=dataset>

Name	Code
Clara cell 10 protein	Cc10
Platelet endothelial cell adhesion molecule	CD31
Estrogen receptor	ER
Hematoxylin and Eosin	H&E
Human epidermal growth factor receptor 2	HER-2
Antigen KI-67	Ki67
Progesterone receptor	PR
Prosurfactant protein C	proSPC

Table 1. Consecutive tissue slices were stained with several different stains.

(ii) appearance differences, and (iii) lack of distinctive appearance objects. Our dataset contains nine tissue samples of three different tissue kinds which form 108 image pairs. For evaluation purposes, we manually placed landmarks, see Table 2. We start with a short description of the particular tissue samples (for stain explanation see Table 1), landmarks and forming registration image pairs.

- **Lung lesion** Unstained adjacent  $3\mu\text{m}$  formalin-fixed paraffin-embedded sections were cut from the blocks and stained with H&E or by immunohistochemistry with a specific antibody for CD31, proSPC, CC10 or Ki67. Images of three mice lung lesions (adenoma or adenocarcinoma) were acquired with a Zeiss Axio Imager M1 microscope (Carl Zeiss, Jena, Germany) equipped with a dry Plan Apochromat objective (numerical aperture  $NA = 0.95$ , magnification  $40\times$ , pixel size  $0.174\mu\text{m}/\text{pixel}$ ).
- **Lung lobes** The images of the four whole mice lung lobes correspond to the same set of histological samples as the lesion tissue. They were also acquired with a Zeiss Axio Imager M1 microscope (Carl Zeiss, Jena, Germany) equipped with a dry EC Plan-Neofluar objective ( $NA = 0.30$ , magnification  $10\times$ , pixel size  $1.274\mu\text{m}/\text{pixel}$ ).
- **Mammary glands** The sections are cuts from two mammary glands blocks stained with H&E (even sections) and alternatively, with an antibody against the ER, PR, or Her2-neu (odd sections). They were also acquired with a Zeiss Axio Imager M1 microscope (Carl Zeiss, Jena, Germany) equipped with a dry EC Plan-Neofluar objective ( $NA = 0.30$ , magnification  $10\times$ , pixel size  $1.274\mu\text{m}/\text{pixel}$ ).

**Landmarks** The landmarks are stored in CSV format, which is very intuitive, and they have standard ImageJ structure and coordinate frame. The origin (0,0) of the coordinate system is set to the image top left corner. Further landmarks are available along with annotation tools<sup>4</sup>, which also provides the possibility to add new landmarks and share them among all dataset users.

<sup>4</sup><https://github.com/Borda/dataset-histology-landmarks>

Name	$\mu\text{m}/\text{pixel}$	# images	# points	Avg. size [pixels]
Lung Lesions 1	0.174	5	78	16k
Lung Lesions 2	0.174	5	101	23k
Lung Lesions 3	0.174	5	80	16k
Lung lobes 1	1.274	5	98	10k
Lung lobes 2	1.274	5	107	10k
Lung lobes 3	1.274	5	80	9k
Lung lobes 4	1.274	5	86	9k
Mammary gland 1	2.294	5	82	22k
Mammary gland 2	2.294	8	76	20k

Table 2. Dataset summary and it properties.

	Cc10	CD31	H&E	Ki67	proSPC
Cc10	-	1	2	3	4
CD31	1	-	5	6	7
H&E	2	5	-	8	9
Ki67	3	6	8	-	10
proSPC	4	7	9	10	-

Table 3. An example of the 10 registration pairs from a set of 5 differently stained images.

**Pairing images** As the stained samples within each set are very close each to other and to increase the number of registration pairs, we register all image to each other. We assume that the registration of two images (target and source) is symmetric  $S \rightarrow T$  and  $T \rightarrow S$ , so we drop duplicates. The benchmarks require a list of these pairing with its landmarks on input.

### 3.3. Experimental setting

We run experiments on Linux server with 24 CPU and 250GB RAM. As it is above standard machine, we run four experiments in parallel. Moreover, the framework has an option to normalise execution time to any other define machine.

As the dataset offers several scales we perform an experiment on WSI (denoted as "full") and also a mix size images close to 10k pixels in image diagonal (denoted as "10k"), the same as ANHIR<sup>5</sup> challenge did.

We set hard time-out limit 3 hours per single image registration; if a method does not finish in time, it is terminated and considered as a fail.

### 3.4. Results

The summary result on both dataset scopes are presented in Table 4. We have observed a vast gap between using 10k and full dataset scope since some methods are not able to work on larger images then 32k pixels and fail. For this reason, we present all visual comparison on the 10k dataset scope, see visualised method comparison from several perspectives in an angular chart in Fig. 2.

In particular, the rTRE distribution and related met-

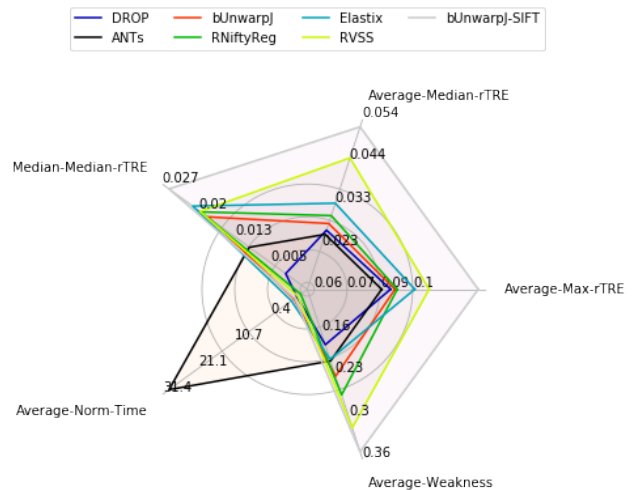


Figure 2. Summary visualisation of benchmark results for all method on 10k scope.

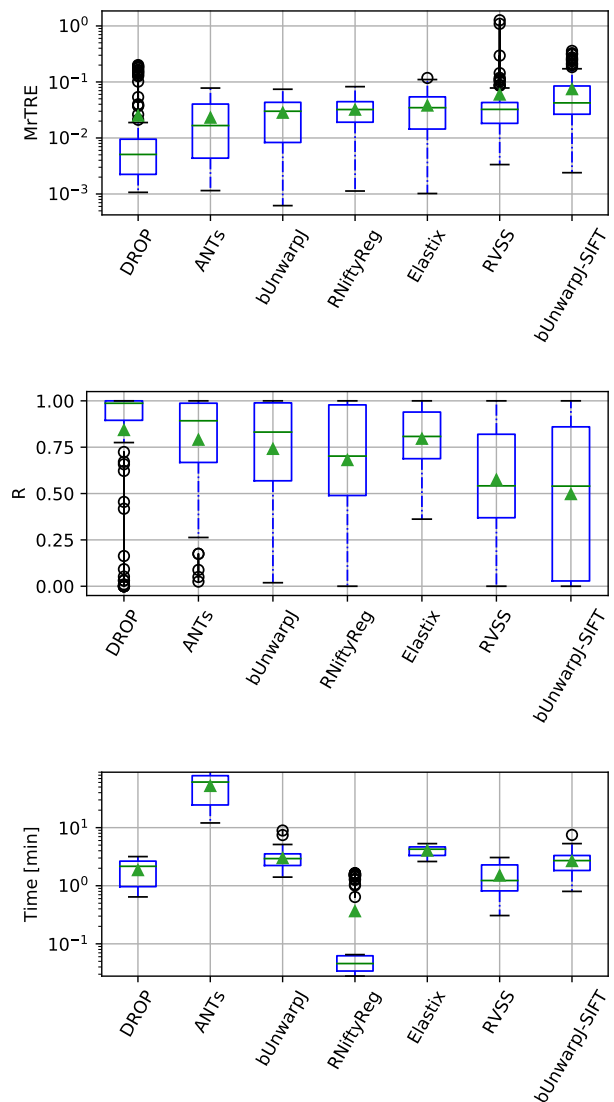


Figure 3. Box visualisation of distribution of (top) Median rTRE, (middle) Robustness and (bottom) execution time on dataset scope 10k.

<sup>5</sup><https://anhir.grand-challenge.org/>

methods	scope	Median rTRE		Max rTRE	Robustness		time
		Average	Median	Average	Average	Median	[min]
ANTs	10k	0.0230	0.0167	0.0556	0.7902	0.8925	52.17
	full	0.0385	0.0347	0.0736	0.3035	0	210.46
DROP	10k	0.0250	0.0051	0.0629	0.8425	0.9868	1.86
	full	0.0281	0.0089	0.0666	0.6123	0.8651	11.71
bUnwarpJ	10k	0.0282	0.0300	0.0666	0.7407	0.8313	2.99
	full	0.0326	0.0336	0.0711	0.6761	0.6881	14.01
RNiftyReg	10k	0.0320	0.0322	0.0685	0.6805	0.702	0.36
	full	0.0316	0.0327	0.0683	0.6977	0.7814	0.39
Elastix	10k	0.0379	0.0347	0.0829	0.7955	0.8077	4.02
	full	0.0411	0.0380	0.0839	0.7061	0.6974	16.92
RVSS	10k	0.0595	0.0324	0.0948	0.5745	0.5412	1.5
	full	0.0403	0.0361	0.0763	0.5513	0.5242	4.59
bUnwarpJ-SIFT	10k	0.0743	0.0423	0.1353	0.4970	0.5401	2.66
	full	0.0590	0.0426	0.1240	0.5097	0.5401	11.36

Table 4. Aggregated results of all methods over both dataset scopes (sizes - 10k pixels and full image size).

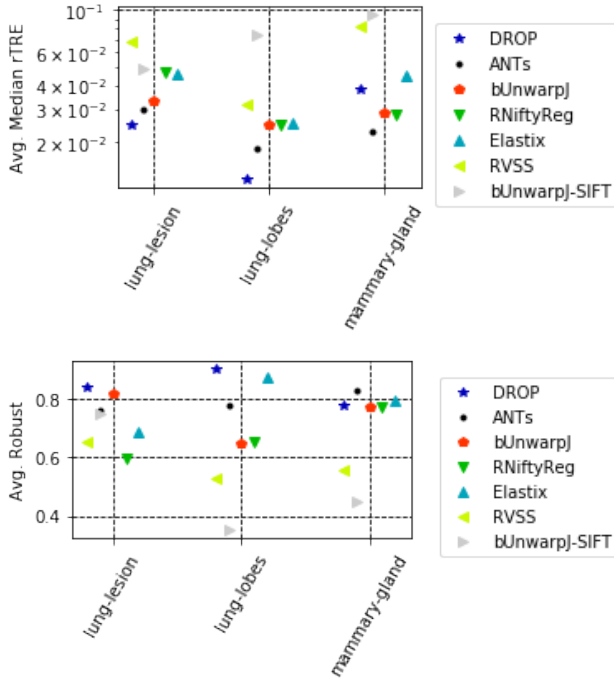


Figure 4. Performance visualisation of particular methods depending on tissue kind: (top) Average Median rTRE and (bottom) Robustness on dataset scope 10k.

rics like Robustness together with execution time are presented in Fig. 3.

From the performed experiment we see the DROP and the best performing method among the limited selection of compared methods.

We have also compared result depending on the tissue kind as they significantly differ in appearance - repetitive texture patterns and tissue separability from the background, see Fig. 4.

## 4. Conclusion

In this report, we briefly introduced the developed image registration framework using datasets with landmark-like annotation and presented the main application use-cases. We described the used histology dataset with necessary information about collected data. Later we presented state-of-the-art integrated methods and their results on the presented dataset so any future work can be compared with these result as a baseline.

## References

- [1] I. Arganda-Carreras, C. Sorzano, R. Marabini, Al., M. José Carazo, C. Ortiz-de Solorzano, and J. Kybic. Consistent and elastic registration of histological sections using vector-spline regularization. In *Computer Vision Approaches to Medical Image Analysis*, volume 4241, pages 85—95, 2006. 3
- [2] B. B. Avants, C. L. Epstein, M. Grossman, and J. C. Gee. Symmetric diffeomorphic image registration with cross-correlation: Evaluating automated labeling of elderly and neurodegenerative brain. *Medical Image Analysis*, 12(1):26–41, 2008. 3
- [3] M. H. Chin, A. B. Geng, A. H. Khan, W. J. Qian, V. A. Petyuk, J. Boline, S. Levy, A. W. Toga, R. D. Smith, R. M. Leahy, and D. J. Smith. A genome-scale map of expression for a mouse brain section obtained using voxelation. *Physiological Genomics*, 30(3):313–321, 2007. 1
- [4] R. Fernandez-Gonzalez, A. Jones, E. Garcia-Rodriguez, P. Chen, A. Idica, S. Lockett, M. Barcellos-Hoff, and C. Ortiz de Solórzano. System for combined three-dimensional morphological and molecular analysis of thick tissue specimens. *Microscopy Research & Techniques*, (59):522–530, 2002. 3
- [5] I. Garcia, G. Mayol, E. Rodríguez, M. Suñol, T. R. Gershon, J. Ríos, N. K. V. Cheung, M. W. Kieran, R. E. George, A. R. Perez-Atayde, C. Casala, P. Galván, C. de Torres, J. Mora, and C. Lavarino. Expression of the neuron-specific protein CHD5 is an independent marker

- of outcome in neuroblastoma. *Molecular Cancer*, 9:1–14, 2010. 1
- [6] B. Glocker, N. Komodakis, G. Tziritas, and N. Navab. Dense image registration through MRFs and efficient linear programming. *Medical Image Analysis*, 12(6):731–741, 2008. 3
- [7] B. Glocker, A. Sotiras, N. Komodakis, N. Paragios, and A.I. Deformable Medical Image Registration: Setting the State of the Art with Discrete Methods. *Annual Review of Biomedical Engineering*, 13(1):219–244, 2011. 3
- [8] G. Haskins, U. Kruger, and P. Yan. Deep Learning in Medical Image Registration: A Survey. 2019. 1
- [9] K. Kartasalo, L. Latonen, T. Visakorpi, M. Nykter, and P. Ruusuvuori. Comparative Analysis of Tissue Reconstruction Algorithms for 3D Histology. *Bioinformatics*, 34(17):2360–2364, 2018. 1
- [10] K. Kartasalo, L. Latonen, T. Visakorpi, P. Nykter, and P. Ruusuvuori. Benchmarking of image registration methods for 3D tissue reconstruction. In *IEEE International Conference on Image Processing*, number 269474, pages 2–6, 2016. 1
- [11] S. Klein, M. Staring, and K. Murphy. Elastix: a toolbox for intensity-based medical image registration. *Medical Imaging, IEEE*, 29(1), 2010. 3
- [12] X. M. Lopez, P. Barbot, Y. R. Van Eycke, L. Verset, A. L. Trépant, L. Larbanoix, I. Salmon, and C. Decaestecker. Registration of whole immunohistochemical slide images: An efficient way to characterize biomarker colocalization. *Journal of the American Medical Informatics Association*, 22(1):86–99, 2014. 1
- [13] D. Lowe. Distinctive image features from scale-invariant keypoints. 60(2):91–110, 2004. 3
- [14] J. B. Maintz and M. A. Viergever. A survey of medical image registration. *Medical image analysis*, 2(1):1–36, mar 1998. 1
- [15] G. J. Metzger, S. C. Dankbar, J. Henriksen, A.I., A. E. Rizzardi, N. K. Rosener, and S. C. Schmechel. Development of multigene expression signature maps at the protein level from digitized immunohistochemistry slides. *PloS One*, 7(3):e33520, jan 2012. 1
- [16] M. Modat, D. Cash, P. Daga, G. Winston, J. S. Duncan, and S. Ourselin. A symmetric block-matching framework for global registration. volume 9034, page 90341D, 03 2014. 3
- [17] K. Murphy, B. Van Ginneken, J. M. Reinhardt, A.I., E. A.I., S. Kabus, K. Ding, X. Deng, K. Cao, K. Du, G. E. Christensen, V. Garcia, T. Vercauteren, N. Ayache, O. Com-mowick, G. Malandain, B. Glocker, N. Paragios, N. Navab, V. Gorbunova, J. Sporring, M. De Bruijne, X. Han, M. P. Heinrich, J. a. Schnabel, M. Jenkinson, C. Lorenz, M. Modat, J. R. McClelland, S. Ourselin, S. E. a. Muenzing, M. a. Viergever, D. De Nigris, D. L. Collins, T. Arbel, M. Peroni, R. Li, G. C. Sharp, A. Schmidt-Richberg, J. Ehrhardt, R. Werner, D. Smeets, D. Loeckx, G. Song, N. Tustison, B. Avants, J. C. Gee, M. Staring, S. Klein, B. C. Stoel, M. Urschler, M. Werlberger, J. Vandemeulebroucke, S. Rit, D. Sarrut, and J. P. W. Pluim. Evaluation of registration methods on thoracic CT: The EMPIRE10 challenge. *IEEE Transactions on Medical Imaging*, 30(11):1901–1920, 2011. 1
- [18] Z. S. Novakovic, M. G. Durdov, L. Puljak, M. Saraga, D. Ljutic, T. Filipovic, Z. Pastar, A. Bendic, and K. Vukovic. The interstitial expression of alpha-smooth muscle actin in glomerulonephritis is associated with renal function. *Medical Science Monitor*, 18(4):235–240, 2012. 1
- [19] S. Ourselin, A. Roche, and G. Subsol. Reconstructing a 3D structure from serial histological sections. *Image and Vision Computing*, 19(1-2):25–31, 2001. 3
- [20] J. Salvi, C. Matabosch, D. Fofi, and J. Forest. A review of recent range image registration methods with accuracy evaluation. *Image and Vision Computing*, 25(5):578–596, 2007. 1
- [21] J. Schindelin, I. Arganda-Carreras, E. Frise, and Others. Fiji: an open-source platform for biological-image analysis. *Nature Methods*, 9(7):676–682, 2012. 3
- [22] Y. Song, D. Treanor, A. Bulpitt, A.I., and D. R. Magee. 3D reconstruction of multiple stained histology images. *Journal of Pathology Informatics*, 4(2):7, 2013. 1
- [23] A. Sotiras, C. Davatzikos, and N. Paragios. Deformable Medical Image Registration: A Survey. *Trans Med Imaging*, 32(7):1153–1190, jul 2013. 1
- [24] P. J. Thul and C. Lindskog. The human protein atlas: A spatial map of the human proteome. *Protein Science*, 27(1):233–244, 2018. 1
- [25] J. West, J. M. Fitzpatrick, and M. Y. Wang. Comparison and evaluation of retrospective intermodality brain image registration techniques. *Journal of Computer Assisted Tomography*, 21(4):554–568, 1997. 1
- [26] B. Zitová, J. Flusser, and B. Zitova. Image registration methods: a survey. *Image and vision computing*, 21(11):977–1000, 2003. 1